Bio-Medical Materials and Engineering 26 (2015) S1587–S1597
DOI 10.3233/BME-151458
IOS Press

Speckle noise reduction in ultrasound images using a discrete wavelet transform-based image fusion technique

Hyun Ho Choi[a], Ju Hwan Lee[a], Sung Min Kim[a] and Sung Yun Park[b,*]
[a]*Department of Medical Biotechnology, Dongguk University-Bio Medi Campus, 32, Dongguk-ro, Ilsandong-gu, Goyang-si, Gyeonggi-do, South Korea*
[b]*Oriental Medicine College, Dongguk University-Gyongju Campus, 123, Dongdae-ro, Gyeongju-si, Gyeongsangbuk-do, South Korea*

Abstract. Here, the speckle noise in ultrasonic images is removed using an image fusion-based denoising method. To optimize the denoising performance, each discrete wavelet transform (DWT) and filtering technique was analyzed and compared. In addition, the performances were compared in order to derive the optimal input conditions. To evaluate the speckle noise removal performance, an image fusion algorithm was applied to the ultrasound images, and comparatively analyzed with the original image without the algorithm. As a result, applying DWT and filtering techniques caused information loss and noise characteristics, and did not represent the most significant noise reduction performance. Conversely, an image fusion method applying SRAD-original conditions preserved the key information in the original image, and the speckle noise was removed. Based on such characteristics, the input conditions of SRAD-original had the best denoising performance with the ultrasound images. From this study, the best denoising technique proposed based on the results was confirmed to have a high potential for clinical application.

Keywords: Ultrasound imaging, speckle noise, image fusion, discrete wavelet transform, SRAD

1. Introduction

Ultrasonography is one of the most popular medical imaging techniques for the visualization of muscles, tendons, and various internal organs due to the fact that it is safe, cheap, and provides real-time tomographic images of specific lesions [1]. This technique is used to diagnose lesions by employing the ultrasound image from the transducer. Reception signals generated by reflections from inside the human body are converted into electrical pulses via a transducer, and converted to the ultrasound image after being sent to the scanner.

A common problem with ultrasonic diagnosis is speckle noise generated from the non-homogenous structure of the tissue, following a Rayleigh distributed noise [2, 3]. Speckle noise is a specific form of noise that degrades fine details and edge definitions in ultrasound images [4]. It also appears as a

* Address for correspondence: Sung Yun Park, Research Institute of Oriental Medicine, Dongguk University-Gyeongju Campus, 123, Dongdae-ro, Gyeongju-si, Gyeongsangbuk-do, South Korea. Tel.: +82-31-961-5608; Fax: +82-31-961-5610; E-mail: bmepark@gmail.com.

granular pattern that does not conform to the microstructure of actual human tissue. The purpose of image filtering is to efficiently remove speckle noise from images, with minimal loss of edges and critical features.

A number of studies have been performed to resolve the speckle noise problem. Thakur, et al. [5] applied the wavelet transform and packets to improve the quality of images affected by the speckle noise generated from ultrasonic images. Damodaram, et al. [6] applied the Wiener filtering technique [7] to remove the speckle noise in ultrasonic images of the liver to improve diagnostic information. Sivakumar, et al. [8] used a filtering technique involving the extraction of edges to minimize the speckle noise generated from ultrasonic images, and to distinguish between the liver, choroid and kidney. Gedam, et al. [9] applied the filtering techniques of Lee [10], Frost [11] and speckle reducing anisotropic diffusion (SRAD) to degraded wavelets and removed the noise from ultrasonic images. Saranya, et al. [12] used the filtering techniques of Lee, Kuan [13], Frost and oriented SRAD [14] in their study for the purpose of improving the quality of images likely to be affected by speckle noise such as ultrasonic images. Despite these attempts, the use of a single filter in the existing studies failed to preserve detailed and edge information in the intra-image. Therefore, most noise removal algorithms display low denoising performance and lower clinical usability when there is speckle noise.

In the present study, the speckle noise in ultrasonic images was removed using an image fusion-based denoising method. The composition of this paper is as follows. Chapter 2 describes wavelet transform, SRAD, image fusion and image evaluation. Chapter 3 compares the experimental results and a discussion is made in Chapter 4. Finally, the conclusion is presented in Chapter 5.

2. Materials and methods

2.1. Image acquisition

Conventional B-mode and harmonic liver ultrasonic images of cysts were analyzed. To conduct a more specific comparison of the noise reduction performance, regions of interest (ROI) measuring 260 x 260 pixels were designated in the original image with a resolution of 640 x 480 pixels (Figure 1). All

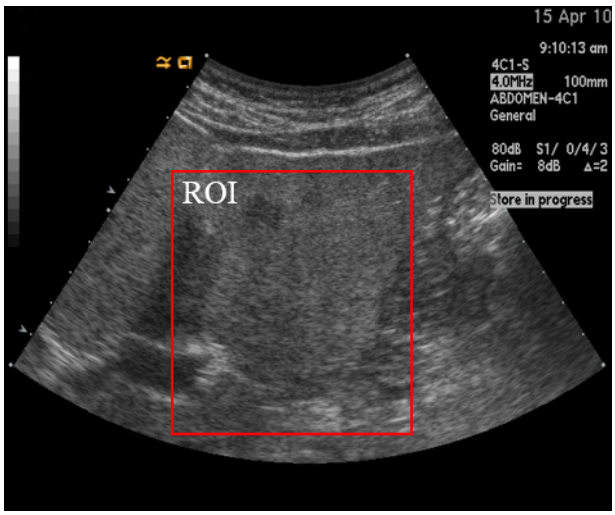

Fig. 1. Ultrasound image's ROI application results.

experimental images were obtained with the ultrasound system, Accuvix V 10 (Samsung Medison Corp., Seoul, Korea).

2.2. SRAD filtering

As anisotropic diffusion performs well with additive Gaussian noise, SRAD [15] is proposed for speckled images without logarithmic compression. SRAD is an edge detector similar to the coefficient of variation of the filter used by Lee [10] and we selected the instantaneous coefficient of variation (ICOV). ICOV is defined as Eq. (1):

$$q = \frac{\sqrt{(\frac{1}{2})(\left|\frac{\nabla I}{I}\right|)^2 - \left(\frac{1}{4}\right)^2 (\frac{\nabla^2 I}{I})^2}}{[1+\left(\frac{1}{4}\right)\left(\frac{\nabla^2 I}{I}\right)]^2} \quad (1)$$

where ∇I represents the image Laplician I. q serves as the edge detector in speckled imagery. ICOV exhibits a high value in edge areas that consist of a high-frequency component, but presents a low value in the same region containing a low-frequency component. Thus it ensures the mean preserving behavior in the homogeneous regions [15, 16]. To this end, SRAD filtered images were utilized as the input images for image fusion algorithm.

2.3. Discrete wavelet transform

A wavelet transform was applied to edges with various sizes to extract them from ultrasound images. Discrete wavelet transform (DWT) uses the scale parameter as well as the shifting parameter for wavelet transformation. The scale parameter either expands or compresses the width of a wavelet function while maintaining its basic structure. The larger a scale value becomes, the greater the width becomes, presenting the features of a low-frequency component. In contrast, the smaller a scale value becomes, the greater the features of a high-frequency component. The shifting parameter determines the position of functions along the time axis. As the value of shifting parameters become larger, the functions move to the right in parallel.

Step 1 DWT decomposes the original image into one approximation image (LL_1) and three detailed images (LH_1, HL_1, HH_1). The LL_1 image contains the low frequency components while LH_1, HL_1 and HH_1 contain the high frequency components in horizontal, vertical and diagonal directions, respectively. The step 2 decomposition process decomposes Step 1 approximation images into one approximation image (LL_2) and three detailed images (LH_2, HL_2, and HH_2). These images are each decomposed into one sub-approximation image (LL_2) and three detailed images (LH_2, HL_2, HH_2) respectively. This means that Step 2 DWT generates 2 sub-approximation images and a total of 6 sub-detail images. This process can be continued until the required amount of detail is reached. When performing each step, the length of the image being decomposed is reduced by half compared to the original step image. Figure 2 presents the image decomposition results of B-mode ultrasonic images used in Step 2 DWT.

2.4. Image fusion

The image fusion technique can synthesize the image for input through a total of 3 processes; decomposition, fusion and reconstruction of the image (Figure 3). Firstly, the 2 input images are

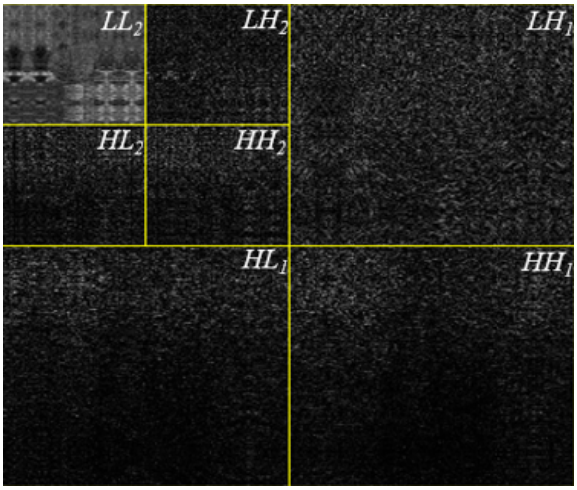

Fig. 2. 2D image decomposition results by DWT (LH_1: 1-level horizontal image, HL_1: 1-level vertical image, HH_1: 1-level diagonal image, LL_2: 2-level approximation image, LH_2: 2-level horizontal image, HL_2: 2-level vertical image, HH_2: 2-level diagonal image).

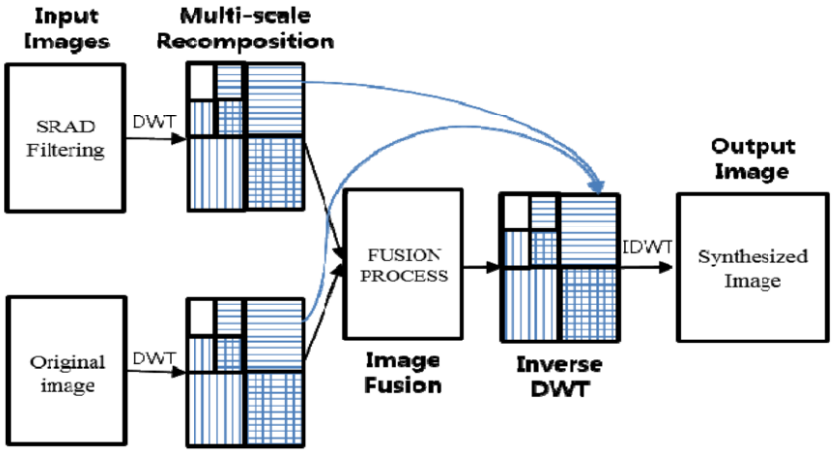

Fig. 3. Multiresolution image fusion scheme.

decomposed into sub-images with high frequency and low frequency through the DWT technique. The low-frequency sub-image is composed of a component associated with the coarse portion of the original image, while the high-frequency sub-image is composed of components corresponding to the boundaries or edges. Next, the fusion process combines the key information from each input image. Wavelet-based image fusion is performed by the sub image element containing details and features of the original image. The purpose of the fusion process is to combine the complementary information via multiple modality images. Thus the principle of creating fusion rules is to retain the characteristics as a new image, without loss of components such as potential regions and edges. To this end, a fusion selection rule is applied to extract the important information [17]. When the absolute value of transformation is larger in the sub-band image, the image presents its characteristics such as rapid intensity variation, edges, lines, and region boundaries. An excellent integration rule selects the larger absolute values among two coefficients of the wavelet transform at each point. Therefore, the fusion

selection rule is defined as Eq. (2).

$$W(x,y) = \begin{cases} W_1(x,y), \text{if } |W_1(x,y)| \geq |W_2(x,y)| \\ W_2(x,y), \text{if } |W_2(x,y)| > |W_1(x,y)| \end{cases} \quad (2)$$

where input images $I_1(x,y)$ and $I_2(x,y)$ are decomposed at different levels using DWT to obtain wavelet coefficients $W_1(x,y)$ and $W_2(x,y)$. Inverse discrete wavelet transform of $W(x,y)$ will provide a fused image. Finally, the fused image is converted to a final image using the selected coefficient and the backward wavelet transform. Through these processes, a synthesized image is derived from two input images.

2.5. Evaluation parameters

To evaluate noise reduction performance, the mean square error (MSE), signal-to-noise ratio (SNR), and peak signal-to-noise ratio (PSNR) were employed. The MSE measures the quality change between the original image and the denoised image, and is widely used to quantify image quality, however it does not correlate strongly with perceptual quality when used alone. It should therefore be used together with other quality metrics and visual perception. The SNR compares the level of the desired signal to the level of background noise. The higher the ratio, the less obtrusive the background noise is. The PSNR is a ratio between the maximum possible power of the signal and the noise content. Higher PSNR values show better image quality. For identical images, the MSE becomes zero and the PSNR is undefined.

$$MSE = \frac{1}{MN}\sum_{i=1}^{M}\sum_{k=1}^{N}(Y-X)^2 \quad (3)$$

$$SNR = 10log_{10}\frac{\frac{1}{MN}\sum_{i=1}^{M}\sum_{k=1}^{N}Y^2}{MSE}\ [dB] \quad (4)$$

$$PSNR = 10log_{10}\left(\frac{255^2}{MSE}\right)\ [dB] \quad (5)$$

where M and N are the number of rows and columns, respectively. X is the original image and Y is the denoised image.

3. Experimental results

3.1. Comparison of noise reduction performance according to the different DWT and filtering schemes

Tables 1 and 2 show the quantitative results of MSE, SNR, and PSNR for the B-mode cyst ultrasound image, according to different DWT and filtering methods. The first image reconstruction level of DWT provided a higher noise reduction performance than the second level (Table 1). Under the first reconstruction level, the DMEY scheme outperformed the other methods, demonstrating the lowest MSE of 48.57, the highest SNR of 21.35 dB and a PSNR of 31.27 dB. The worst performing method in terms of MSE, SNR, and PSNR was the BIOR method (Table 1).

Analysis of existing methods revealed that the SRAD scheme had the most significant noise reduction performance (MSE=29.90, SNR=23.46 dB, and PSNR=33.37 dB), while the Median

Table 1

Quantitative results of MSE, SNR, and PSNR for the B-mode ultrasound image across different decomposition levels of DWT

	MSE		SNR (dB)		PSNR (dB)	
	1 Level	2 Level	1 Level	2 Level	1 Level	2 Level
BIOR	65.81	129.70	20.03	17.09	29.95	27.00
DB	55.94	115.98	20.74	17.57	30.65	27.49
SYM	55.94	115.98	20.74	17.57	30.65	27.49
COIF	54.93	114.92	20.82	17.61	30.73	27.53
DMEY	48.57	108.00	21.35	17.88	31.27	27.80

Table 2

Quantitative results of MSE, SNR, and PSNR for the B-mode ultrasound image according to different filtering methods

	MSE	SNR (dB)	PSNR (dB)
Median	112.81	17.69	27.61
Gaussian	111.59	17.74	27.65
Lee	88.15	18.76	28.68
Frost	49.49	21.27	31.19
SRAD	29.90	23.46	33.37

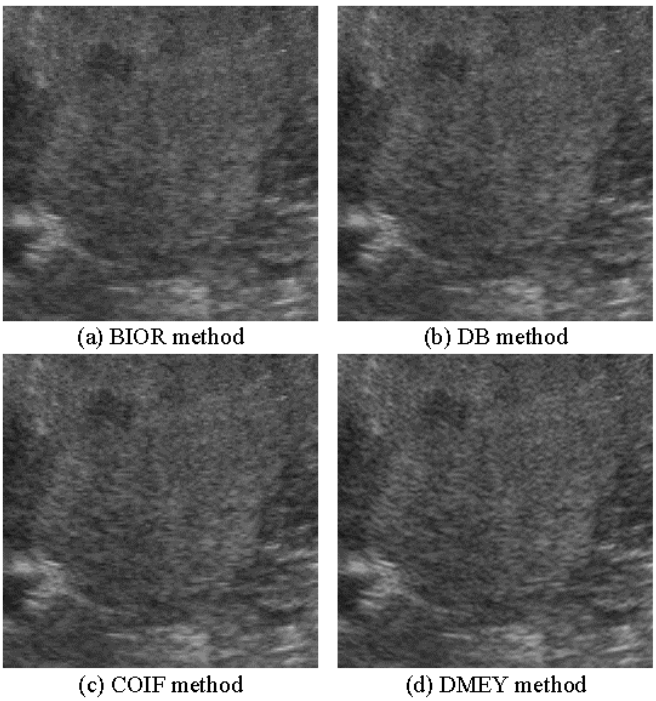

Fig. 4. Speckle noise reduction of a B-mode ultrasound image using the different DWT approaches.

filtering method had the lowest (MSE=112.81, SNR=17.69 dB, and PSNR=27.61 dB). The same results were obtained for analysis of harmonic liver ultrasound images.

Figures 4 and 5 illustrate the noise reduction results for the B-mode cyst ultrasound images using

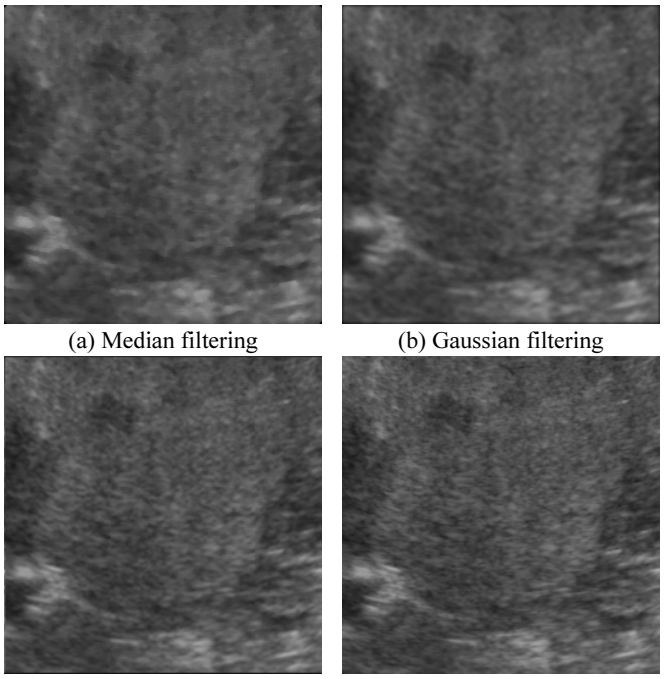

(a) Median filtering (b) Gaussian filtering

(c) Lee filtering (d) SRAD filtering

Fig. 5. Speckle noise reduction of a B-mode ultrasound image using different filtering methods.

various DWT and filtering techniques. BIOR, DB and COIF methods presented a subtle difference in each edge definition. However, the DMEY method greatly preserved the edge of the lesion compared with the other three methods. Median and Gaussian filters showed the loss of edge information and a blurring effect. This result was slightly improved using the Lee filter. The SRAD filter showed outstanding performance compared with the methods mentioned above.

3.2. Comparison of noise reduction performance for different input conditions and decomposition levels during the image fusion procedure

Tables 3 and 4 show different denoising performances according to the input conditions and wavelet levels for the B-mode and Harmonic ultrasound images, respectively. The speckle denoising performance according to different input conditions were high, in the order of SRAD-original > original-SRAD > SRAD-SRAD. SRAD-SRAD had the lowest performance for all the assessment

Table 3

Quantitative results of MSE, SNR, and PSNR for the B-mode ultrasound image across different decomposition levels of DMEY

Input condition	MSE		SNR (dB)		PSNR (dB)	
	1Level	2 Level	1 Level	2 Level	1 Level	2 Level
SRAD-SRAD	30.00	30.00	23.46	23.46	33.37	33.37
Original-SRAD	22.37	29.97	24.72	23.45	34.63	33.36
SRAD-Original	8.88	1.26	28.73	37.19	38.65	47.11

Table 4

Quantitative results of MSE, SNR, and PSNR for the harmonic ultrasound image across different decomposition levels of DMEY

Input condition	MSE		SNR (dB)		PSNR (dB)	
	1Level	2 Level	1 Level	2 Level	1 Level	2 Level
SRAD-SRAD	20.71	20.71	25.15	25.15	34.97	34.97
Original-SRAD	10.33	20.26	28.17	25.24	37.99	35.06
SRAD-Original	11.75	1.80	27.61	35.75	37.43	45.57

methods, MSE, SNR and PSNR. These results were partially enhanced by the 1-level condition of the original-SRAD method, however in the 2nd level, the denoising performance was still significantly lower. Converesely, the 2-level conditions of SRAD-original had the most excellent performance for all input conditions. These results were equal for both B-mode and harmonic images (Tables 3 and 4).

Figures 6 and 7 show the denoised images according to different input conditions for the B-mode and harmonic images, respectively. The Blurring effect appeared in SRAD-SRAD conditions by applying image fusion. However, SRAD-original condition improved fine details and edge definition. The same results were obtained for the analysis of harmonic ultrasound images (Figure 7).

4. Discussion

In the present study, new DWT and image fusion based denoising techniques were proposed to

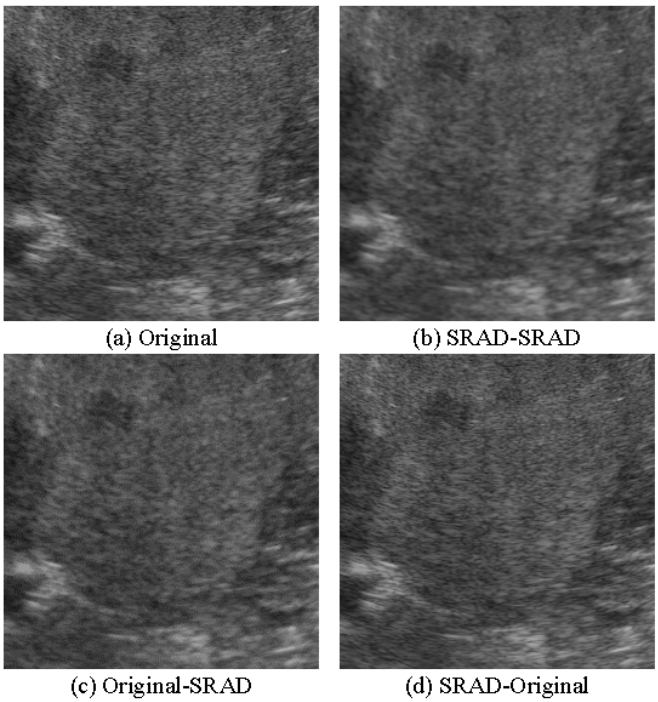

Fig. 6. Speckle noise reduction of a B-mode ultrasound image using the image fusion.

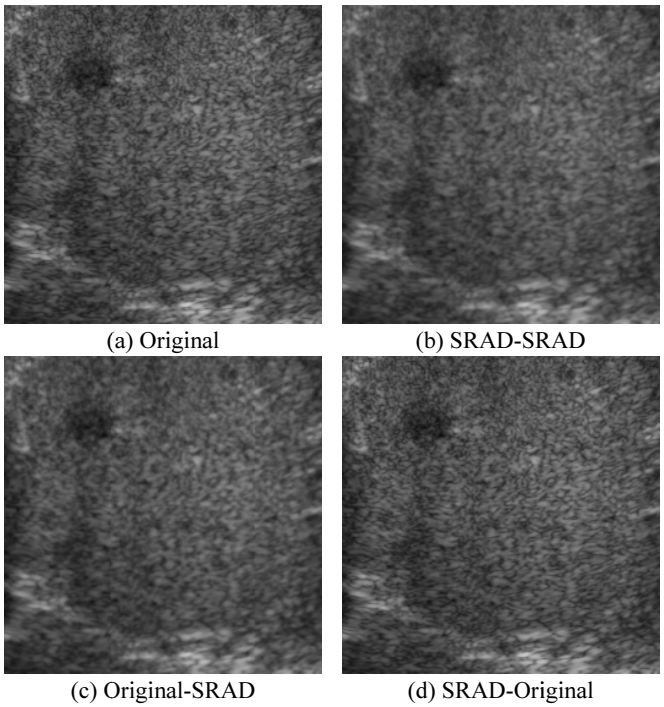

(a) Original (b) SRAD-SRAD

(c) Original-SRAD (d) SRAD-Original

Fig. 7. Speckle noise reduction of a harmonic ultrasound image using the image fusion.

remove the speckle noise in ultrasound images. To optimize the denoising performance of the proposed techniques, the denoising performances for each different DWT and filtering technique were analyzed and compared. In addition, the performances based on different input conditions were compared in order to derive the optimal input conditions. When the denoising performances of different DWT methods and level conditions were compared, the DMEY method had the best performance among all the methods applied. In addition, the 1-level approximation image had better denoising performance than the 2-level approximation image. Such results are due to differences in information loss from the original image. Generally, the 2-level approximation image maximizes the textural information but significantly reduces information in the original image. Therefore, most lesion classification studies extracted the features of the lesion from the 2-level approximation image and assessed the diagnostic accuracy accordingly. Conversely, the experimental results for the 1-level approximation image had a better performance in respect to noise removal. The SRAD filtering technique had the best performance among all the filtering techniques applied. Speckle noise is characterized as multiplicative noise, but existing filtering techniques are unable to remove this noise. SRAD processes the data directly to preserve information in the image, unlike existing filtering techniques, which process the log–compressed [15]. SRAD can control the noise appropriately based on such characteristics, and accordingly, SRAD had the best performance among all of the filtering techniques applied. Based on these results, SRAD and DMEY (DWT) methods were applied to the process of image fusion.

When the denoising performance of various image fusion techniques were compared according to different input conditions, the results were in the order of SRAD-original > original-SRAD > SRAD-SRAD. The original images are typically used as input images for image fusion in CT and MRI. Wang,

et al. [18] used the original image as the input image for image infusion in CT and MRI images in order to measure the location and enlargement of a brain tumor. Angoth, et al. [19] used the original image as the input image to detect the size and position of a brain tumor in CT and MRI images. However, in this study, to measure speckle noise reduction performance, the image used was acquired by applying a SRAD filter to the original image. SRAD-original input conditions from the experimental results were confirmed to exhibit a better denoising performance in ultrasound images. SRAD filtering can remove speckle noise without modifying the image information or losing edge information [15]. To this end, it was determined that the speckle noise was removed by a fusion selection process, but the key information in the original image was clearly preserved. Based on such characteristics, the input conditions of SRAD-original had the best denoising performance with ultrasound images.

5. Conclusions

The experimental results of this study present techniques that exhibited the best denoising performance for speckle noise in ultrasound images. In addition, SRAD-original conditions had the best denoising performance with ultrasound images among all the input conditions tested. From this study, the best denoising technique proposed based on the results, was confirmed to have a high potential for clinical application. Future studies are planned to evaluate the denoising performance by a variety of image types and DWT levels in order to further secure the significance of the experimental results.

Acknowledgment

This work was supported by International Collaborative R & D Program funded by the Ministry of Knowledge Economy (MKE), Korea. (N01150049, Developing high frequency bandwidth (40-60 MHz) high resolution image system and probe technology for diagnosing cardiovascular lesion)

References

[1] Y.S. Kim and J.B. Ra, Improvement of ultrasound image based on wavelet transform: Speckle reduction and edge enhancement, Proceedings of SPIE Medical Imaging **5747** (2005), 1085–1092.
[2] J.G. Abbott and F.L. Thurstone, Acoustic speckle: Theory and experimental analysis, Ultrasonic Imaging **1** (1979), 303–324.
[3] J. Herment, P. Guolielmi, P. Dumee, P. Peronneau and P. Delouche, Limitations of ultrasound imaging and imaging restoration, Ultrasonics **25** (1987), 267–273.
[4] B. Burckhardt, Speckle in ultrasound B-Mode scans, IEEE Trans Sonics and Ultrasonics **25** (1978), 1–6.
[5] Thakur and R.S. Anand, Image quality based comparative evaluation of wavelet filters in ultrasound speckle reduction, Digital Signal Process **15** (2005), 455–465.
[6] N. Damodaran, S. Ramamurthy, S. Velusamy and G.K. Manickam, Speckle noise reduction in ultrasound biomedical B-scan images using discrete topological derivative, Ultrasound in Medicine & Biology **38** (2012), 276–286.
[7] N. Wiener, Extrapolation, Interpolation and Smoothing of Stationary Time Series, MIT Press, One Rogers Street Cambridge MA 02142-1209 USA, 1949.
[8] R. Sivakumar, M.K. Gayathri and D. Nedumaran, Speckle filtering of ultrasound B-scan images-A comparative study between spatial and diffusion filters, IEEE Conference on Open Systems, 2010, Kuala Lumpur, Malaysia, pp. 80–85.
[9] M. Gedam, H. Amrutia and N. Mandal, Biomedical ultrasound image enhancement using SRAD, International Journal of

Applied Information Systems **2** (2013), 38–42.
[10] J.S. Lee, Digital image enhancement and noise filtering by using local statistics, IEEE Transactions on Pattern Analysis and Machine Intelligence **2** (1980), 165–168.
[11] V.S. Frost, J.A. Stiles, K.S. Shanmugan and J.C. Holtzman, A model for radar images and its application to adaptive digital filtering of multiplicative noise, IEEE Transactions on Pattern Analysis and Machine Intelligence **4** (1982), 157–166.
[12] M. Saranya and C. Saraswathy, Speckle reduction in Ultrasound image, International Journal of Electronics and Computer Science Engineering **1** (2012), 343–347.
[13] D. Kuan, A. Sawchuk, T. Strand and P. Chavel, Adaptive restoration of images with speckle, IEEE Transactions on Acoustics, Speech and Signal Processing **35** (1987), 373–383.
[14] K. Krissian, C-F Westin, R. Kikinis and K. Vosburgh, oriented speckle reducing anisotropic diffusion, IEEE Transactions on Image Processing **16** (2007), 1412–1424.
[15] Y. Yu and S.T. Acton, Speckle reducing anisotropic diffusion, IEEE Transactions on Image Processing **11** (2002), 1260–1270.
[16] R. Vanithamani and G. Umamaheswari, Performance analysis of filters for speckle reduction in medical ultrasound images, International Journal of Computer Applications **12** (2010), 23–27.
[17] S. Li, B. Yang and J. Hu, Performance comparison of different multi-resolution transforms for image fusion, Information Fusion **12** (2011), 74–84.
[18] X. Wang, L. Li, C. Hu, J. Qiu, Z. Xu and Y. Feng, A comparative study of three CT and MRI registration algorithms in nasopharyngeal carcinoma, Journal of Applied Clinical Medical Physics **10** (2009), 3–10.
[19] V. Angoth, C. Dwith and A. Singh, A novel wavelet based image fusion for brain tumor detection, International Journal of Computer Vision & Signal Processing **2** (2013), 1–7.